Biosensors and Bioelectronics 195 (2022) 113650

Contents lists available at ScienceDirect

Biosensors and Bioelectronics

journal homepage: www.elsevier.com/locate/bios

Detection of transdermal biomarkers using gradient-based colorimetric array sensor

Jingjing Yu [a,c,1], Di Wang [a,d,1], Vishal Varun Tipparaju [a], Wonjong Jung [b], Xiaojun Xian [a,c,*]

[a] Center for Bioelectronics and Biosensors, The Biodesign Institute, Arizona State University, USA
[b] Photonic Device Lab., Device Research Center, Samsung Advanced Institute of Technology, Samsung, Electronics Co., Ltd., Suwon-si, Gyeonggi-do, 16678, Republic of Korea
[c] Department of Electrical Engineering and Computer Science, South Dakota State University, Brookings, SD, 57007, USA
[d] Intelligent Perception Research Institute, Zhejiang Lab, Hangzhou, 311100, China

ARTICLE INFO

Keywords:
Transdermal volatile biomarkers
Dietary macronutrients intake
Colorimetric sensor
Breath biomarkers
Wearable device

ABSTRACT

Accurate assessment of dietary macronutrients intake is critical for the effective management of multiple diseases, such as obesity, diabetes, cardiovascular disease, metabolic disease, and cancer. Conventional self-reporting method is burdensome, inaccurate, and often biased. Though blood analysis and breath analysis can provide evidence-based information, they are either invasive or subject to human errors. Here we reported a wearable transdermal volatile biomarkers detection system based on novel colorimetric sensing technology for dietary macronutrients intake assessment. This technique quantifies the emission rates of transdermal volatile biomarkers via a gradient-based colorimetric array sensor (GCAS). The optical system of the GCAS device tracks the localized color development associated with the chemical reaction between the volatile biomarkers and the porous sensing probes, and determines the biomarkers emission rates through image processing algorithms. The localized chemical reaction and the image-based signal processing also make the GCAS capable for multiplexed detection of multiple analytes simultaneously. The GCAS sensor has been applied for transdermal acetone detection on 5 subjects in a keto diet intervention. The study indicates that the transdermal acetone increases after the subjects consuming keto diets and it decreases to basal level after intaking carb-rich diets. The transdermal acetone response from the GCAS sensor correlates well with breath acetone concentration in the range between 0 and 40 ppm and the correlation factor (R^2) is as high as 0.8877. This method provides a noninvasive, low-cost, and wearable tool for assessing dietary macronutrients intake outside of lab or hospital settings. It could be widely applied in disease management, weight control, and nutrition management.

1. Introduction

Dietary macronutrients intake is highly associated with our health and lifespan (Fontana and Partridge, 2015; Solon-Biet et al., 2015). Imbalanced dietary macronutrients intake increases the risk of developing multiple diseases, such as obesity, diabetes, cardiovascular disease, metabolic disease, and cancer (Alhazmi et al., 2012; Astrup, 1999; Franceschi et al., 1998; Hu et al., 2015; Kereliuk et al., 2017; Muzio et al., 2007; Organization, 2003). Studies show that following the food intake guideline (Lupton et al., 2002) can significantly reduce risk of these diseases, but reliable and convenient tracking the macronutrients is challenging. Currently self-reporting by hand or by smartphone apps is the primary method to track one's macronutrients intake (Basiotis et al., 1987; Darby et al., 2016). This method has many drawbacks, such as user's burden, and inaccurate and biased record, which lead to incomplete and, often, misleading results (Natarajan et al., 2010). It is reported that the prevalence of under-reporting of dietary macronutrients intake ranges from 18 to 54% in large nutritional surveys (Macdiarmid and Blundell, 1998). In contrast, the methods that can assess dietary macronutrients intake through biomarkers monitoring provide evidence-based information for clinical intervention and effective prevention of various chronic diseases (Combs et al., 2013). This can be achieved by detecting biomarkers presented in body fluids, such as urine and blood (Gibbons and Brennan, 2017; Hedrick et al., 2012). Although more accurate, these methods require frequent collection and analysis of urine or blood samples and using sophisticated analytical equipment,

* Corresponding author. Center for Bioelectronics and Biosensors, The Biodesign Institute, Arizona State University, USA.
E-mail addresses: xiaojun.xian@asu.edu, xianxj@gmail.com (X. Xian).
[1] These authors contributed equally.

https://doi.org/10.1016/j.bios.2021.113650
Received 22 July 2021; Received in revised form 9 September 2021; Accepted 15 September 2021
Available online 20 September 2021

making them difficult for widespread adoption and only available for clinic and lab settings (Hedrick et al., 2012; Potischman, 2003). New sensing technologies are needed for quantitative and noninvasive tracking of biomarkers associated with dietary macronutrients intake.

Volatile compounds released from the human body carry important information about the metabolic processes of human body (Amann et al., 2014; Gallagher et al., 2008; Shirasu and Touhara, 2011). Some volatile biomarkers are correlated with dietary macronutrients intake (Havlicek and Saxton, 2009; Rondanelli et al., 2019). Multiple studies have demonstrated that endogenous acetone is correlated with fat metabolism (Anderson, 2015; Güntner et al., 2018; Landini and Bravard, 2009; Musa-Veloso et al., 2002). Studies also showed that ammonia is correlated with protein metabolism (Petrus et al., 2017; Spacek et al., 2018). Breath hydrogen is generated when bacteria in the colon are exposed to sugars and carbohydrates (Douwes et al., 1980; Ghoshal, 2011; Kotler et al., 1982). Tracking these volatile biomarkers can provide valuable information about dietary macronutrients intake (Avallone et al., 2010; Nose et al., 2005; Prabhakar et al., 2014). Due to their volatility, these molecules are present both in skin via insensible perspiration and in breath (Amann et al., 2014; Naitoh et al., 2002). Studies show that the concentrations of these volatile biomarkers are strongly correlated in skin, blood and exhaled breath (Kondo et al., 2002; Naitoh et al., 2002; Nose et al., 2005; Yamane et al., 2006). Though volatile biomarkers have been intensively studied through blood analysis and breath analysis, the intrinsic issues of these two methods limit their applications. Blood analysis is invasive and requires complex sample processing. Breath analysis is not suitable for continuous monitoring, and breathing pattern change can cause inaccurate measurement of exhaled biomarkers (King et al., 2010). Preferably, a wearable device that monitors volatile biomarkers on skin is more practical for end consumers to assess their dietary macronutrients intake in free-living conditions in a noninvasive and continuous manner.

Challenges need to be overcome for developing a wearable device that can track volatile biomarkers from skin. Firstly, due to the ultra-low emanating rate of volatile biomarkers from the skin (Mochalski et al., 2014), the concentrations of the volatile biomarkers in the skin gas samples can be as low as a few tens of ppb (parts per billion) (Kondo et al., 2002; Yamane et al., 2006). This is why skin gas needs to be collected in a gas sampling bag or pre-concentrator before being analyzed by sophisticated equipment such as high-performance liquid chromatography (HPLC), gas chromatography (GC) and flame ionization detector (Naitoh et al., 2002; Sekine et al., 2007; Yamada et al., 2015; Yamane et al., 2006). In addition to low detection limit, building a wearable device to detect transdermal biomarkers requires a miniaturized sensor with high selectivity and low energy consumption. The mainstream small format gas sensors include metal-oxide semiconductor (MOX), electrochemical and colorimetric sensors. The selectivity of commercially available MOX gas sensors is inadequate to differentiate different chemicals (e.g., acetone vs. alcohol), and the detection limit is insufficient to monitor low-concentration transdermal volatile biomarkers without pre-concentrators (Yamada et al., 2015). Moreover, the MOX sensors operate at elevated temperatures, which makes the device very power-hungry. Electrochemical gas sensors also have selectivity issue. Plus, they are bulky and expensive for wearable devices, and not suitable for multiple volatile biomarkers detection. Both MOX and electrochemical sensors drift over time, and thus must be calibrated periodically in order to maintain acceptable accuracy, adding both cost and burden to the end users.

On the other hand, volatile biomarkers could also be sensitively and selectively detected through colorimetric sensors. Colorimetric sensors detect a color change associated with a specific chemical reaction between an analyte and sensing materials. Besides its low cost, colorimetric sensors are capable for parallel sensing of multiple analytes when used in an array format. Unfortunately, because most colorimetric reactions are irreversible, today's commercial colorimetric sensors are typically for one-time use and for qualitative or semiquantitative analysis only. To overcome the challenges of existing colorimetric sensors, our group has developed technologies to tracking the spatial color distribution to extend the lifetime of the colorimetric sensors (Lin et al., 2018; Tao et al., 2019). But these technologies are adapted to sense airborne chemicals in the environment, where the analytes concentrations are relatively high, the analytes are abundant in the air, the potential interferents are known, and the detection is independent of sensor size. As for detecting transdermal volatile biomarkers, the sensors must be able to capture the analytes secreted and released from the skin in a tiny space, where the concentrations of the analytes are very low and the available analyte molecules to be detected are limited. Challenges also originate from the slow process of volatile biomarkers released from the skin, the highly humid environment, and the high demand for miniaturization of the sensor.

Here we reported the development of a wearable transdermal volatile biomarkers detection system based on novel colorimetric sensing technology for dietary macronutrients intake assessment. As a proof of concept, we demonstrated the feasibility of using this wearable sensing system for keto diet intake monitoring by continuously monitoring the transdermal acetone emission. The detection is achieved by quantifying the emission rates of acetone via a gradient-based colorimetric array sensor (GCAS). The GCAS tracks the localized color development associated with the chemical reaction between the volatile biomarkers and the porous sensing probes. The detection can be achieved in two ways: 1) processing the optical images of the GCAS before and after the volatile biomarkers exposure; 2) processing the real-time optical signal of the GCAS during the volatile biomarkers exposure for continuous monitoring. The localized chemical reaction and the image-based signal processing also make the GCAS capable for multiplexed detection of multiple analytes simultaneously. This method provides a noninvasive, low-cost, and wearable tool for assessing dietary macronutrients intake outside of lab or hospital settings. It will have wide applications in disease management, weight control, and nutrition management.

2. Material and methods

2.1. Materials

Acetone sensing solution was prepared by dissolving 100 mg Hydroxylamine sulfate (CAS 10039-54-0, 99.999%, Sigma–Aldrich 379913) and 10 mg thymol blue (CAS 76-61-9, Honeywell Fluka 32728) into a mixture of 6.5 mL water and 3.5 mL methanol. The pH of the acetone sensing solution was adjusted to 5 using 1 M sodium hydroxide solution. 40 mg bromophenol blue (CAS 115-39-9, Sigma–Aldrich B0126) was dissolved into a mixture of 5 mL water and 5 mL ethanol for ammonia sensing. Carbon dioxide sensing solution was prepared by dissolving cresol purple (CAS 62625-31-4), glycine (CAS 56-40-6), and hexadecytrimethlyammonium hydroxide (CAS 505-86-2) into water, and ethanol according to literature report (Bridgeman, 2017). Cobalt chloride hexahydrate (CAS 7791-13-1, >98%, TCI C2388) was used to indicate humidity level. Ultrapure water (18 MΩ*cm) was produced via an ELGA Purelab Ultra RO system. Ethanol (99.5%), and methanol (99.9%) were purchased from Sigma-Aldrich. Silica gel TLC plates (200 μm, polyester backed, catalog#: 1624026, TLC: thin layer chromatography) purchased from Sorbent Technologies, Inc. was used as the substrate of sensor chip. The calibration gas of 100 ppm acetone, 300 ppm ammonia was purchased from Gasco, and diluted with clean air to low concentration for testing. 4% and 7.6% standard carbon dioxide calibration gas was used for CO_2 sensing.

Ketogenic (or keto) diet contained fat-rich foods including heaving whipping cream and sausage, and other foods including pistachio, shrimp, strawberry and grape tomato. The ratio of food was adjusted to satisfy personal taste as long as the energy percentage from different macronutrients remains the same. 80%, 5% and 15% energy percent were from fat, carbohydrate, and protein, respectively. An example for detailed keto diet composition can be reviewed in the Supplementary

Material (Table S2). Carbohydrate-rich (carb-rich) diet was bread or noodle, in which more than 55% energy was from carbohydrates.

2.2. Colorimetric sensor chip fabrication

Sensor chips (Figs. 2A and 4D) were prepared by cutting TLC plate into certain shapes with a laser cutter (Universal VLS3.50). Sensing solutions were drawn on TLC plate with Lamy Safari fountain pen (L17EF) and vacuum dried for 1 min for offline sensor chip (Fig. 2A). Then a tape was used to cover the top of the chip. For the online sensor chip (Fig. 4D), sensing solutions were cast on TLC plate and vacuum dried for 15 min. Each sensing channel had a dimension of 0.8 mm × ~5.5 mm × 200 μm. Only the porous silica in the sensing channel regions was kept on the sensor chip and sensors were covered with transparent tape (adhesive Scotch Transparent Tape from 3 M) on top (Fig. S5).

2.3. Experimental setup and methods

For bench test (Fig. 2E and F), the offline sensor chip was put in a gas chamber filled with target gas samples for 6 h. Pictures before and after gas exposure were captured and absorbance difference (Δabsorbance) was calculated (Fig. S1). The offline sensor chip was attached on the skin directly with 3 M medical materials 1522 polyethylene double coated tape for skin biomarkers test. The color of sensor chip after 6 h test was captured by phone camera. Selected ion flow tube mass spectrometer (SIFT-MS) was used as reference instrument for skin gas monitor, and the detection with SIFT-MS was performed after sensor chip attached on skin for around 3 h. The sampling bag was connected to the inlet of the SIFT-MS, and the transdermal gases released from the forearm was collected by the sampling bag and then diffused into SIFT-MS. Fig. S2 shows a typical SIFT-MS signal of in-situ skin tests.

While for the test of online sensor chip (Fig. 4D and E), the sensor chip was fixed in the device and the color of chip was recorded with Logitech C525 webcam in real-time through reflection mode (Fig. 4C). The artificial gas was introduced into the device to check the feasibility of sensor chip at the flow rate of 0.6 L/min (Fig. 5). The flowing gas will diffuse into sensor channel and react with sensing material. The device was worn on the wrist of the subject (Fig. 4A) to detect transdermal volatile biomarkers. The regions of interest were selected for data processing and absorbance calculation (Fig. S6).

Typically, each online skin test lasted for 1 h with fresh GCAS chip (Figs. 6 and 7). The continuous long-time test lasted for around 4 h (Fig. 8A). Ketoscan mini analyzer, an FDA-approved device, was used as reference sensors to detect breath acetone, and the average value during the skin test period were used as reference. The performance of the Ketoscan mini analyzer was validated against blood ketone analyer and a very good correlation was found between the blood ketone levels and the breath acetone levels (Fig. S3 in Supplementary Materials). Breath acetone can be detected by blowing breath gas into Ketoscan mini analyzer directly. The heart rate and blood oxygen saturation (SpO_2) were also recorded during online skin test with CMS60D pulse oximeter (Table S4 in Supplementary Material).

2.4. Subjects for online skin test

5 healthy and non-smokers subjects without regular medication, history of respiratory diseases and diabetes were recruited to participate in the pilot study. Physiological and metabolic parameters of these subjects can be reviewed in the Supplementary Material (Table S3). The study was approved by the Institutional Review Board of Arizona State University (IRB reference protocols number STUDY00013474). All the subjects participated in the study voluntarily and signed consent form before the tests. Disposable mouth pieces were used for breath gas analysis. Before the test of skin volatile biomarker, the forearm skin was cleaned with water and dried with wipers. The diet-control test lasted two days. The detail of the diets and testing time of each subject can be found in the Figs. 6C and 7A-7D).

3. Results and discussion

3.1. Sensing principle of gradient-based colorimetric array sensor (GCAS) for transdermal volatile biomarkers detection

The sensing principle of detecting transdermal volatile biomarkers using the gradient based colorimetric array sensor (GCAS) is illustrated in Fig. 1. Transdermal volatile biomarkers are emitted from the skin (Fig. 1A) and then diffused into the opening of the porous GCAS sensing channel (Fig. 1B). The biomarker reacts selectively with the sensing probes in the channel and specific color change starts to develop. A color gradient is formed in the channel along with this colorimetric chemical reaction and the diffusion of the biomarkers in the porous channel. The speed of the color gradient movement is correlated with the emission rate of the transdermal volatile biomarkers. Given an exposure time, the distance of the color development in the sensing channel is correlated with the emission rate of the volatile biomarkers released from the skin, as shown in Fig. 1C. The key components of the GCAS system include 1) a GCAS sensor chip that can localize and visualize the color development associated with the chemical reaction between the transdermal volatile biomarkers and the porous sensing probes; and 2) an optical readout that can measure the optical signal caused by the localized color development to quantitatively determine the emission rates of the transdermal volatile biomarkers. The sensor chip can be designed to have multiple gradient sensing channels with different colorimetric sensing probes loaded on a porous matrix for multiple transdermal volatile biomarkers detection. The porous matrix is essential to localize the gas-solid phase reaction between the transdermal biomarkers and sensing probes within the gradient sensing channels to produce color gradient. Our group has developed a gradient tracking algorism by using image processing method (Lin et al., 2018). In this study, considering the color development in the channel is relative slow process in skin gas detection, we found that this gradient tracking algorithm can be significantly simplified by defining two sensing regions (reacting region and intact region) along the channel and using the absorbance to quantify the analyte. This will reduce the data processing burden on the MCU (microprogrammed control unit), facilitating the real-time

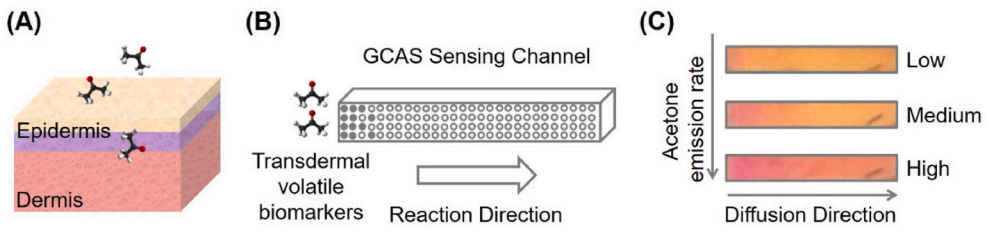

Fig. 1. Schematic illustrating the gradient based colorimetric array sensor (GCAS) for transdermal biomarkers detection. (A) Emission of biomarkers from skin. (B) Schematic illustrating color gradient generated on the colorimetric sensing channel under transdermal volatile biomarkers exposure. (C) Color gradient developed in the colorimetric sensing channel under different emission rates of skin acetone exposure. (For interpretation of the references to color in this figure legend, the reader is referred to the Web version of this article.)

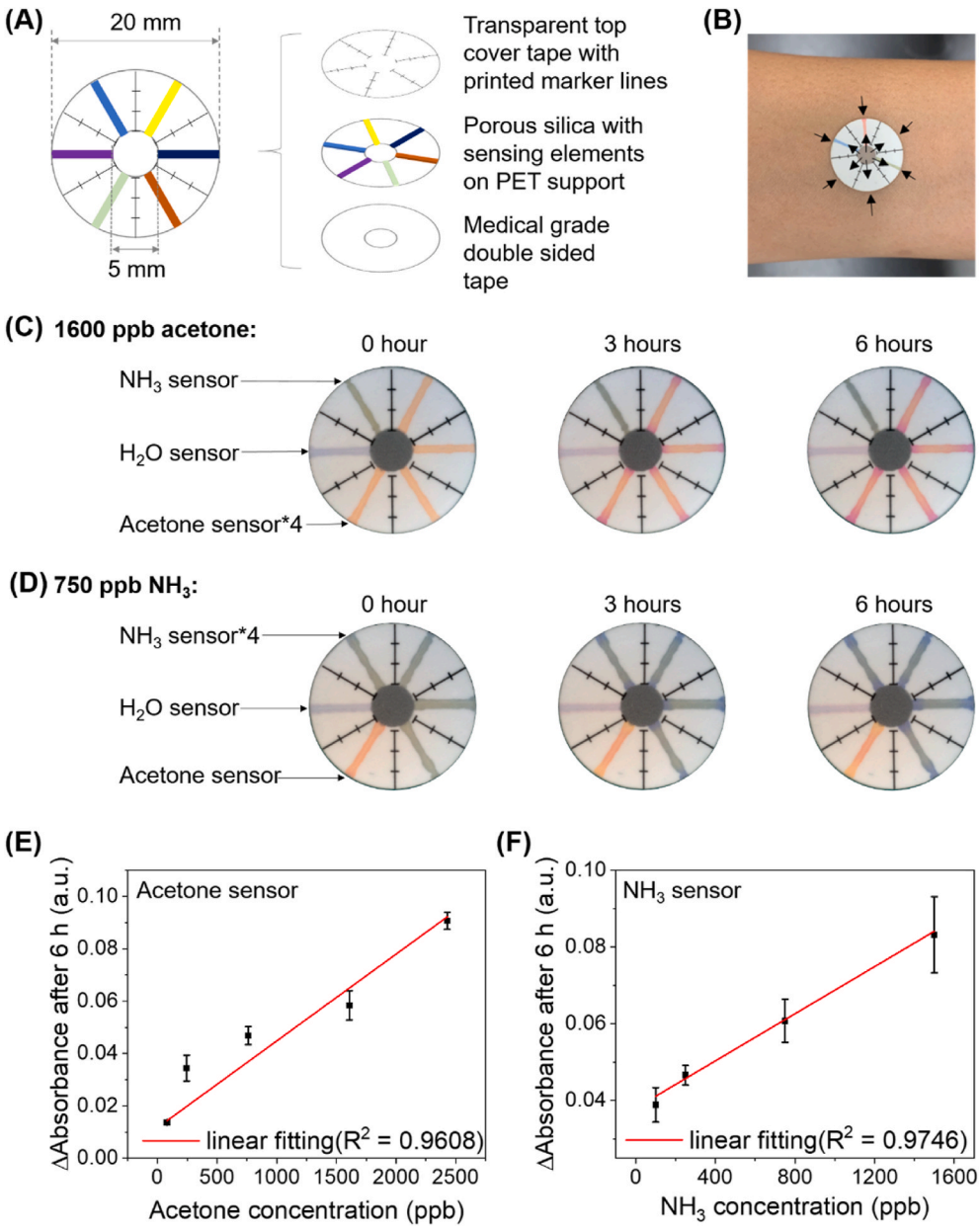

Fig. 2. (A) Schematic illustrating the structure of the GCAS sensor chip for offline detection of transdermal volatile biomarkers. Totally 6 gradient sensing channels are implemented in this design. (B) Image of a GCAS attached to forearm. The arrows indicate the direction of gas diffusion. (C) The images of one GCAS before and after exposure to acetone. 4 gradient sensing channels showed "pink-yellow" color gradients after exposure to acetone. (D) The images of one GCAS before and after exposure to NH_3. 4 gradient sensing channels showed "blue-green" color gradients after exposure to NH_3. (E) The calibration plot of GCAS for acetone detection. (F) The calibration plot of GCAS for NH_3 detection. The error bars correspond to the standard deviations of four sensors after 6 h gas exposure. (For interpretation of the references to color in this figure legend, the reader is referred to the Web version of this article.)

tracking capability of the sensor. We have compared the methods of absorbance change (in this research) and gradient tracking (our previous paper), and a very good correlation between these two methods have been observed (Supplementary Material Fig. S11).

Through the combination of localized chemical reaction and the image-based optical signal processing, the GCAS can achieve multiplexed detection of multiple transdermal volatile biomarkers simultaneously, as shown in the following sections. Though the emission rate of transdermal volatile biomarker is very low, the porous GCAS sensing channel can serve as a preconcentrating column to accumulate the color development over time, which is essential to provide enough sensitivity for the transdermal biomarker detection. The colorimetric detection can be passively achieved without using any fan or pump for gas delivery, which saves power for the wearable system. Since the metabolism of the macronutrients is a slow process (in the hour scale), the emission rate of transdermal volatile biomarker changes slowly. This physiological feature allows the response time of the skin gas sensor can be relatively slow. This is in the favor of the GCAS sensing because the sensor will have enough time to accumulate the color development, and thus improve its sensitivity. There are two ways to quantify the optical signal from the GCAS sensor chip: 1) offline mode, in which the GCAS sensor chip is attached to skin for transdermal volatile biomarkers exposure and then image the exposed sensor chip by a camera for signal processing and emission rate determination; 2) online mode, in which the GCAS sensor chip is integrated into a wearable device with miniaturized optical imager for real-time signal processing. The results of these two sensing modes are presented below.

3.2. *Offline detection of transdermal volatile biomarkers of macronutrients intake by using GCAS*

As shown in Fig. 2A and B, the GCAS sensor chip can be constructed by implementing multiple gradient sensing channels on the same substrate with a shared opening at the center and outside edge. The transdermal volatile biomarkers can diffuse into each gradient sensing channel from the opening and cause localized color development. When needed, a gas permeable membrane can be integrated upon the central opening to let selective gases passing through the membrane to enhance

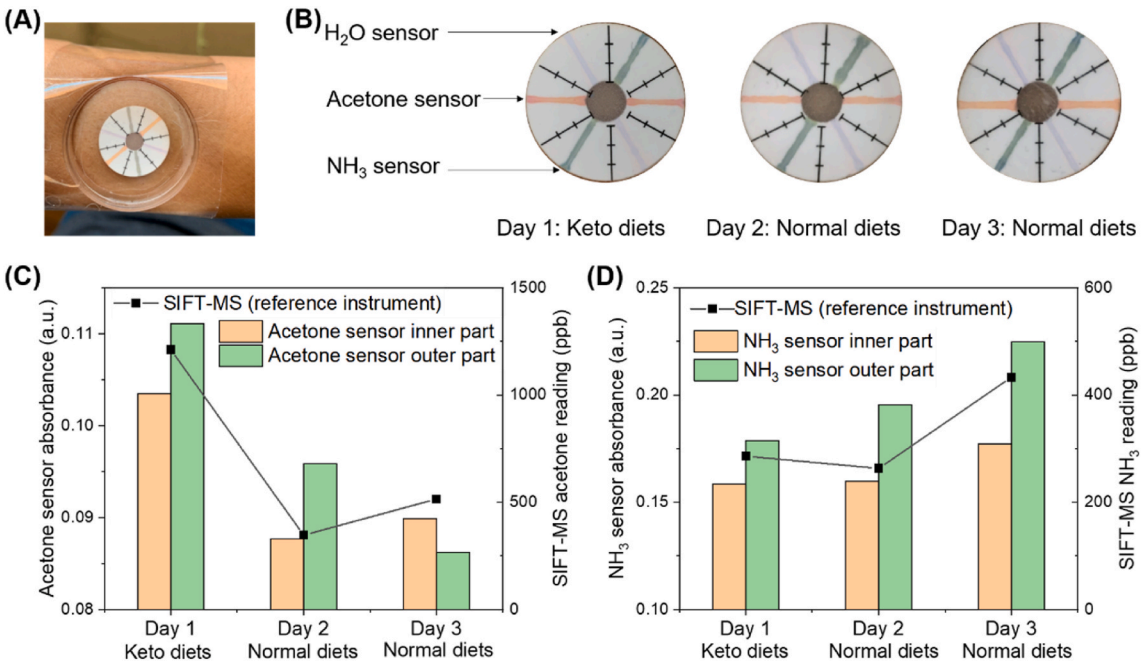

Fig. 3. The results of in-situ detection of transdermal gases. (A) The image of a GCAS attached to the forearm for in-situ detection of transdermal gases. A transparent chamber is covered on top to block possible ambient interferences. (B) The photos of the GCASs with H_2O, acetone, and NH_3 gradient sensing channels after 6 h of wearing in the 3 days tests. (C) The correlation between the results from GCAS and reference instrument (SIFT-MS) for in-situ detection of transdermal acetone. (D) The correlation between the results from GCAS and reference instrument (SIFT-MS) for in-situ detection of transdermal NH_3. After ketogenic diets, skin acetone level rose above 1 ppm in day 1.

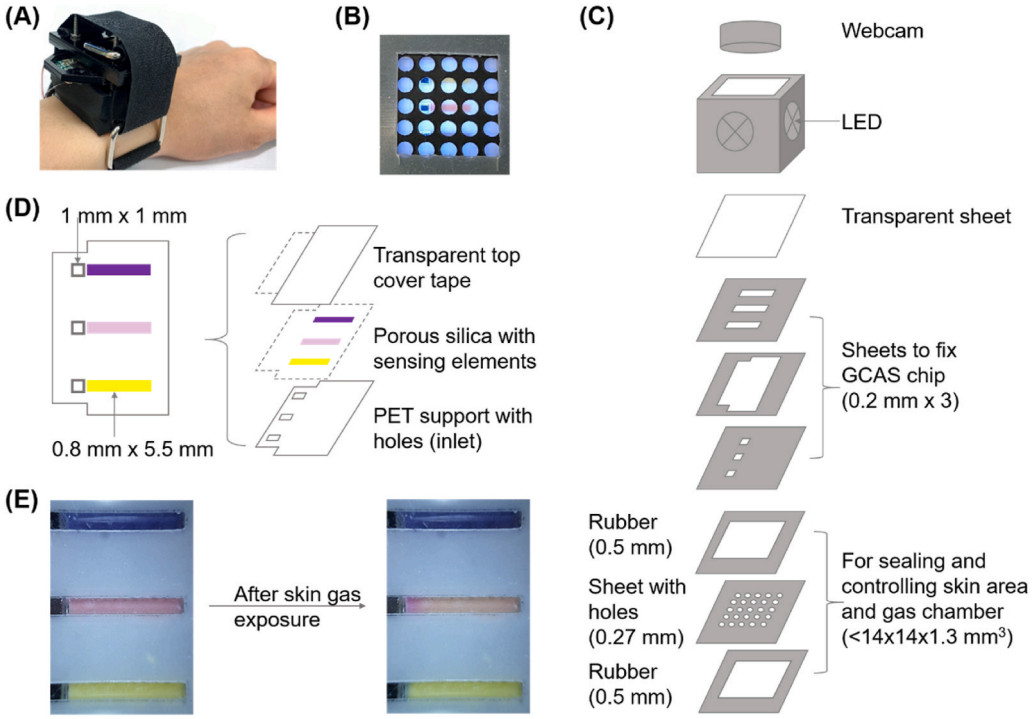

Fig. 4. Wearable wristband device and GCAS sensor chip for transdermal biomarkers detection. (A) Images of the wearable wristband device. (B) Bottom view of the device. An array of holes was made on the plastic sheet for transdermal biomarkers diffusion. (C) Schematic of the wristband device. (D) Schematic of GCAS sensor chip (E)GCAS sensor chip with CO_2, acetone and NH_3 sensing channels before and after transdermal biomarkers exposure after keto diets.

the selectivity of the GCAS. For instance, a hydrophobic membrane could be applied to reduce the humidity interference to the GCAS. Sensing channels were formed by coating colorimetric sensing elements onto the porous silica substrate. Totally 6 gradient sensing channels are implemented by coating different colorimetric sensing solutions on a porous silica substrate. Transparent top cover tape (ZICOTO premium printable water-resistant vinyl sticker paper) with printed marker lines was adhered to the silica substrate to facilitate the visualization of the

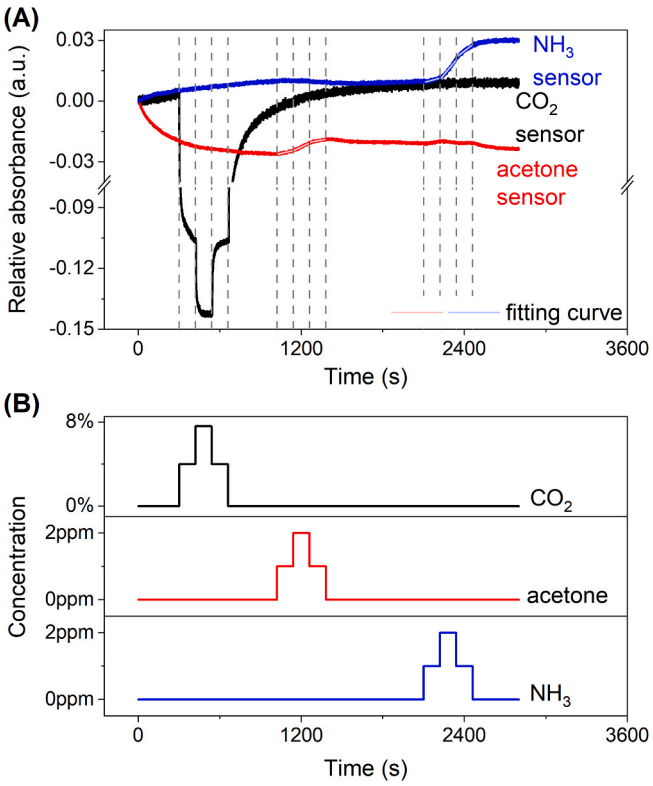

Fig. 5. Sensing performance of GCAS sensor chip to different concentrations of analytes. (A) Real-time color change of different sensors were recorded at the same time during the test in accordance to (B) different concentrations of different gases. Black curve: 0%, 4%, 7.6% CO_2. Red curve: 0 ppm, 1 ppm, 2 ppm acetone. Blue curve:0 ppm, 1 ppm, 2 ppm NH_3. Gas was humidified to higher than 90% RH (25 °C). Relative absorbance is obtained from the region of interest (ROI), defining as the first 1/3 of the entire sensing channel with initial intensity as reference. (For interpretation of the references to color in this figure legend, the reader is referred to the Web version of this article.)

color development along the sensing channel. The marker lines can be used for two purposes: a) marking of the sensor positions and b) its black color and the substrate's white color can be used in color balancing to compensate the variation caused by various light conditions when taking pictures with camera phone. A medical-grade double-sided tape was used to provide an air-tight adherence of the GCAS sensor chip on the skin. The holes in the centers of silica substrate and the double-sided tape, together with the top cover tape form a small gas chamber, which allows transdermal gases to diffuse into the GCAS. Fig. 2B is an image of a GCAS attached to forearm. In this GCAS sensor chip, the color development starts at the opening position of the sensing channels. As the exposure time increases, the color development extends along the horizontal channel and the position of the maximum color gradient moves. Through image processing algorithms, the spatial information of the maximum color gradient can be extracted and then the emission rate of the volatile transdermal biomarkers can be determined by applying the calibration factors. To simplify the data processing, the color change of regions of interest in the channel instead of spatial gradient information was used to determine the gas emission rate.

Fig. 2C shows the images of one GCAS sensor chip before and after exposure to acetone. 4 gradient sensing channels showed "pink-yellow" color gradients after exposure to acetone. Fig. 2D shows the images of one GCAS sensor chip before and after exposure to NH_3. 4 gradient sensing channels showed "blue-green" color gradients after exposure to NH_3. Fig. 2E shows the calibration plot of GCAS sensor chip for acetone detection. Fig. 2F shows the calibration plot of GCAS sensor chip for NH_3 detection. Humidified gas samples in these tests were used to simulate the humid condition on top of skin. Acetone sensor and NH_3 sensor showed obvious color changes after they were exposed to target analytes. Green channel and red channel were used to analyze acetone sensors and NH_3 sensors, respectively. The region used to analyze the color was described in Fig. S1. Calibration results show that the sensors have wide dynamic ranges. A humidity sensor is integrated into the GCAS sensor chip, which can be used to correct humidity effect and may also be used to detect skin hydration level and sweating.

Preliminary in-situ skin tests were performed on a human subject for 3 days using the GCAS sensor chip, including 1 day after ketogenic diets and 2 days of normal diets. The GCAS sensor chip was prepared with two acetone sensors, two NH_3 sensors and two humidity sensors. The GCAS sensor chip was attached to the subject's forearm and covered by a transparent chamber to block possible ambient interferences (Fig. 3A). A smartphone was used to take pictures of the GCAS sensor chip after the transdermal volatile biomarkers exposure. Each day, transdermal acetone and NH_3 were tested by a reference instrument, selected ion flow tube mass spectrometer (SIFT-MS). SIFT-MS is capable of detecting multiple analytes simultaneously in real time, which is an ideal reference instrument for in-situ skin tests. Fig. 3B are the photos of the GCAS with H_2O, acetone, and NH_3 gradient sensing channels after 6 h of wearing in the 3 days tests. There were two sensors for each analyte on the same GCAS sensor chip, and the averaged absorbances were used as the GCAS sensing results. Fig. 3B indicates that the humidity levels of the sensors become saturated and constant after being placed on skin, due to the fast insensible perspiration of the skin. This result rules out errors induced by humidity change, and eliminates the need of integrating humidity sensors in the GCAS sensor chip for the wearable wristband device. The humidity detected from Sensirion SHTx3 humidity sensor also indicates that the humidity level can be saturated quickly in 5 min (Fig. S8A). Sweating may influence the detection. However, sweating was not observed underneath the sensor after wearing 6 h because the experiments were carried out in a cool (~25 °C) and dry (~20% RH) laboratory environment, and the subjects were in the resting condition. Fig. 3C shows the correlation between the results from GCAS and reference instrument (SIFT-MS) for in-situ detection of transdermal acetone. Fig. 3D shows the correlation between the results from GCAS and reference instrument (SIFT-MS) for in-situ detection of transdermal NH_3. The results show that there is a good correlation between the GCAS sensors and the reference instrument SIFT-MS. The high skin acetone level in day 1 after ketogenic diets supports that transdermal gases could be useful biomarkers for diet monitoring. Different from acetone, ammonia level in day 1 was not significantly different from day 2 and day 3, because the protein intake during keto diet and normal diet was similar.

3.3. *Online detection of transdermal biomarkers of macronutrients intake by using GCAS*

Online detection of transdermal biomarkers was achieved by integrating the GCAS sensor chip into a wearable device (Fig. 4A) with an optical imager for real-time signal recording. As shown in Fig. 4C, the wearable wristband had three major components: the light source, the GCAS sensor chip, and the webcam imager. A white LED array was integrated into the sensing chamber to illuminate the GCAS sensor chip. An array of holes was fabricated on the plastic sheet to allow transdermal volatile biomarkers diffusing to the GCAS sensor chip, as shown in Fig. 4B. The GCAS sensor chip was located between the gas diffusion sheet and the webcam imager. The small gas chamber formed between the gas diffusion sheet and the GCAS sensor chip had a dimension of 14 mm (width) × 14 mm (length) × 1.3 mm (height). This small dimension was important to build up the concentration of biomarkers in a confined space. The webcam imager was able to capture real-time images of the GCAS sensor chip, from which the optical signals (e.g., intensity, absorbance) from the red, green, blue channels could be processed and analyzed through a home-made Matlab program. Webcam imagers also

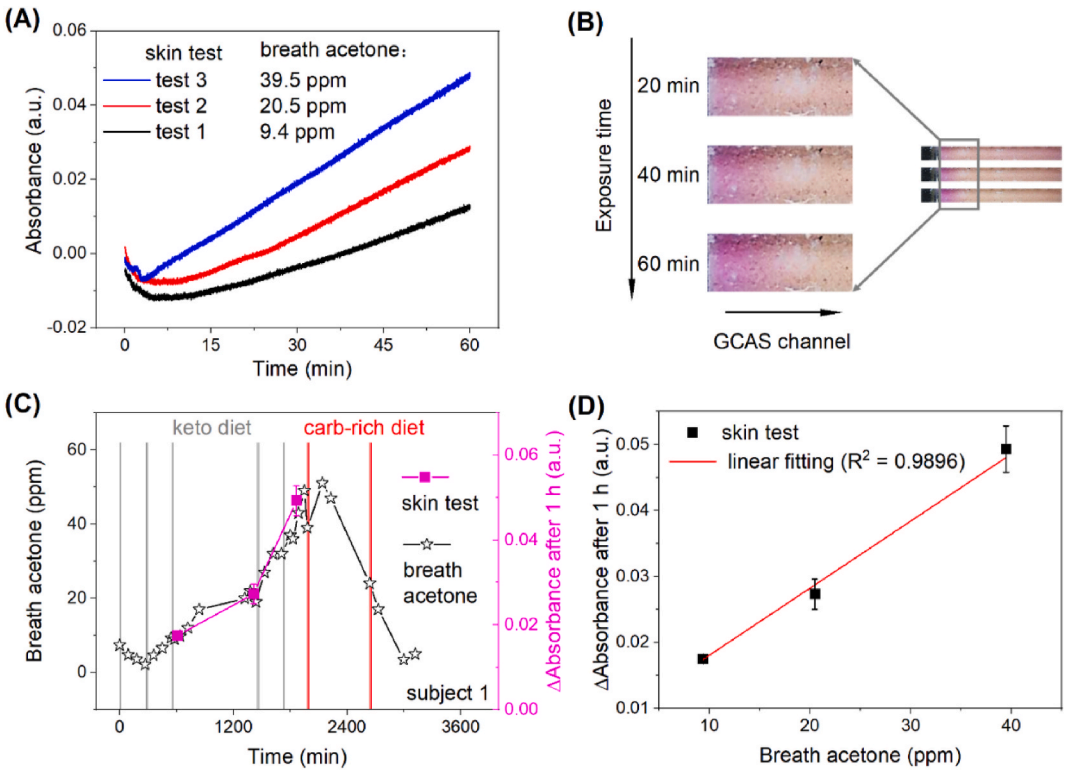

Fig. 6. GCAS sensor for online transdermal acetone test. (A) Real-time optical absorbance (green channel) of GCAS sensor for skin acetone detection. (B) Screenshots of color development along the GCAS sensing channel in 1 h duration (the corresponding breath acetone concentration was 39.5 ppm). The contrast and white balance was adjusted for clarity. (C) Profiles of breath acetone levels and transdermal acetone response from GCAS sensor in the diet-control test. Keto diet and carb-rich diet were introduced to modulate acetone level in breath and skin. The gray lines indicate the time for taking keto diet and red lines indicate the time for taking carb-rich diet. (D) Correlation of GSAS sensor signal and breath acetone (R-square = 0.9896). The error bars correspond to the standard deviations of three regions. (For interpretation of the references to color in this figure legend, the reader is referred to the Web version of this article.)

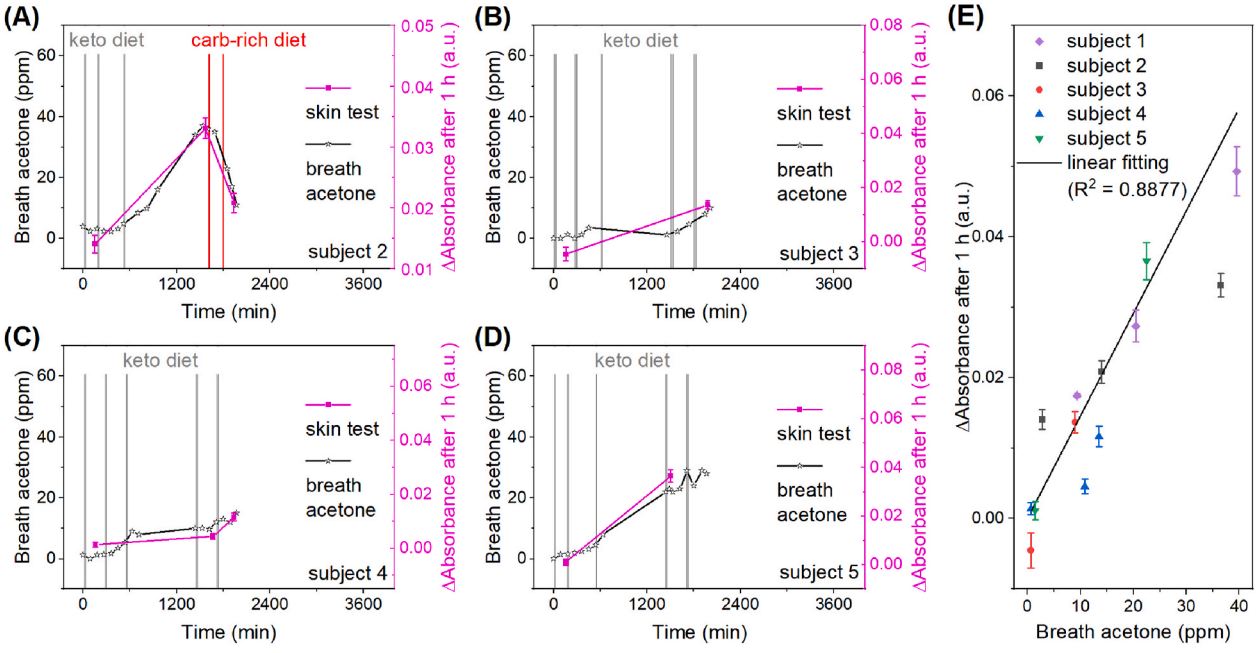

Fig. 7. Validation of GCAS sensor for skin transdermal acetone detection against corresponding breath acetone for different subjects. Keto diet and carb-rich diet were introduced to modulate acetone level in breath and skin of the subjects. (A) Subject 2 (B) subject 3 (C) subject 4 (D) subject 5. The gray lines indicate the time for taking keto diet and red lines indicate the time for taking carb-rich diet. (E) Correlation between transdermal acetone detected by GCAS sensor and breath acetone levels for all human subjects in the diet-control test. The error bars correspond to the standard deviations of three regions. (For interpretation of the references to color in this figure legend, the reader is referred to the Web version of this article.)

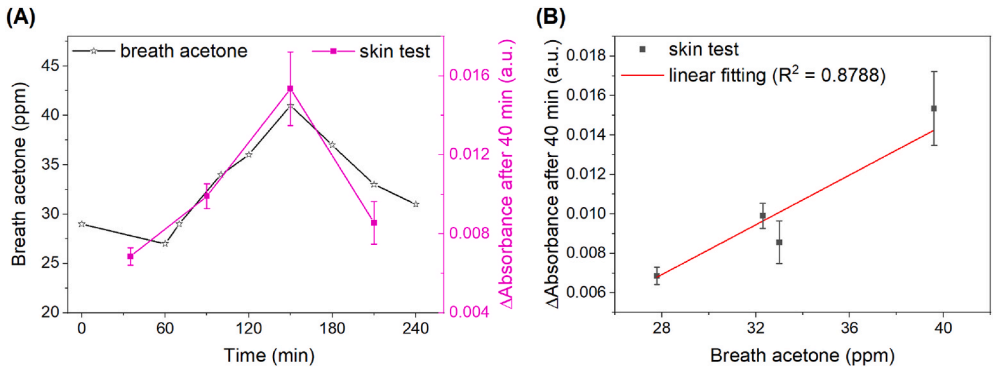

Fig. 8. Continuously tracking of transdermal acetone with the same GCAS sensor chip in a 4-h test. (A) Profiles of breath acetone levels and GCAS sensor response in a keto diet intervention study. (B) The correlation plot between breath acetone levels and GCAS sensor response. The error bars correspond to the standard deviations of three regions.

allowed simultaneous monitoring of multiple sensing channels on the GCAS sensor chip. In the current design, there were three sensing channels on the GCAS sensor chip, one for acetone, one for ammonia, and one for carbon dioxide. The GCAS sensor chip was fabricated by coating three kinds of sensing solutions onto TLC plate to form three separate sensing channels. After coating and drying, a transparent top cover tape was applied to the TLC substrate to isolate the sensing channels from each other to avoid gas leakage from the side of the channels. A small opening (gas inlet) was fabricated at one end of each sensing channel to allow transdermal volatile biomarkers to diffuse in (Fig. 4D). Fig. 4E showed the images of the GCAS sensor chip before and after 1 h exposure of transdermal volatile biomarkers using the wearable wristband device after keto diets. It's obvious that the localized color development occurred in acetone sensing channel (middle), suggesting the design of the GCAS sensor chip and wearable wristband device were effective.

The performance of the GCAS sensor chip and wearable wristband device was tested with artificial analyte gases in clinically relevant ranges. Sensor chip integrated with acetone, CO_2 and NH_3 sensors (Fig. 4D) were put into the device for simultaneous detection of acetone, CO_2, and NH_3. The color changes of these three sensors were recorded at the same time as shown in Fig. 5A. Different concentrations of CO_2, acetone, and NH_3 were introduced into the device as shown in Fig. 5B. Fig. 5A indicated a negligible cross-sensitivity among different sensors. The absorbance of acetone sensor decreased first (red curve in Fig. 5A), due to the humidified gas introduced to the sensor, but it became stable after 10 min. The humidity interference on acetone sensor was discussed in Supplementary Material (sections 9 and 10). For irreversible sensors, such as acetone and NH_3 sensor, the absorbance of the region of interest (ROI) changed at a constant rate under a fixed gas concentration (red and blue curves in Fig. 5A). The higher the analyte concentration, the faster the absorbance rate. While for reversible CO_2 sensor (Black curve in Fig. 5A), When the gas concentration was switched from low to high, a dramatic absorbance decrease happened and finally reached the saturated absorbance. The absorbance difference (Δabsorbance) before and after gas exposure in a fixed time can be used to determine the gas concentrations of both reversible and irreversible sensors.

We tested the performance of the GCAS sensor chip and wearable wristband device on a human subject with diet intervention. Keto diets were introduced to boost the acetone level of the subject in breath and skin. Considering the close correlation between breath acetone and skin acetone, an FDA-approved breath acetone analyzer testing breath acetone was used as a reference sensor for validating the skin acetone level tested with GCAS. Compared to SIFT-MS, the breath acetone analyzer was much cheaper and easy-to-use for tracking the acetone profile of the subject. As for skin acetone detection, the fully assembled wristband device was worn on the subjects' forearm for 1 h for each test. Three skin tests were performed when the averaging breath acetone levels reached 9.4 ppm, 20.5 ppm and 39.5 ppm (9 ppm and 9.8 ppm, 22 ppm and 19 ppm, 36 ppm and 43 ppm at the beginning and the end of the transdermal acetone test, 1 h duration). Fig. 6A showed the real-time absorbance of the ROI from the green channel during this 1 h test (green channel gave the most sensitive response compared to the red and blue channels). The absorbance from green channel decreased first because of humidity influence from skin and then kept increasing, indicating the continuous color development in the sensing channel. Fig. 6B illustrated the screenshots of the sensing channel at different time of the test, which showed a very clear progressive color development along the sensing channel in this 1-h test. The paired transdermal acetone and breath acetone test at different stages of the keto diet intervention test were performed. The correlation between the transdermal acetone response from the GCAS device and the breath acetone concentration from the reference analyzer was plotted in Fig. 6C and D. A linear correlation with the R-square of 0.9896 was observed. Since studies have shown that the concentrations of volatile biomarkers are strongly correlated in skin, blood and exhaled breath (Kondo et al., 2002; Naitoh et al., 2002; Nose et al., 2005; Yamane et al., 2006), these test results proved the effectiveness of our GCAS sensor and wearable wristband device for transdermal biomarkers detection.

We further evaluated the performance of the wearable GCAS wristband device for transdermal acetone detection in a diet-control pilot study on another four healthy subjects. The diet-control study was designed as following: 1) checking the baseline breath acetone before the diet intervention was implemented; 2) introducing keto diet to boost the acetone level in breath; 3) Introducing carb-rich diet to bring down the acetone level if breath acetone was close to 40 ppm (Figs. 6C and 7A). Due to the slow dietary metabolism process, the entire study section lasted for roughly two days. The detection of acetone from skin was performed 2 or 3 times for each subject. Fig. 7A–D showed the profiles of breath acetone levels and transdermal acetone response from GCAS sensor from each subject in this diet-control pilot study. The keto diet effectively increased the acetone levels of all subjects, and the breath acetone level reached as high as 37 ppm from a baseline level of 2.3 ppm for subject 2. The keto diet showed difererent effect on different subjects. Some subjects had a faster rate of acetone level increasing while others were relatively slow. The carb-rich diet could effectively bring the acetone level down. The good correlation between the GCAS sensor responses and the breath acetone concentrations were observed for all the subjects at each stage of the test. Fig. 7E showed the correlation between the transdermal acetone response from the GCAS device and the breath acetone concentrations from the breath analyzer for all subjects. Transdermal acetone response from the GCAS wristband device correlated well with the corresponding acetone concentration in breath for all the subjects, and the R-square of the correlation plot was 0.8877.

We also explored the capacity of the GCAS sensor chips for long-time continuous tracking of transdermal acetone in keto diet and carb-rich

diet intervention (diets-control pilot similar as Fig. 7A). Similar to the procedures described in the previous section, a subject consumed keto diets to boost the acetone level and carb-rich diets to decrease acetone level in breath and skin. The subject wore the wristband device and the same GCAS sensor chip was used for continuous tracking of transdermal acetone in a time duration of 4 h. The breath acetone concentrations were measured periodically. Both breath acetone levels and response from the same GCAS sensor chip were plotted in Fig. 8A. The GCAS response followed the trend of the breath acetone level change very well. We should point out that considering the low emission rate of skin biomarkers and the excess sensing materials in the channel, the emitted acetone will be consumed by the sensing materials. So there is a dynamic equilibrium between the biomarker emission and consumption. The good correlation between breath and skin acetone indicates the equilibrium is quick enough to monitor the skin acetone continuously. Fig. 8B showed the correlation plots of the breath acetone levels and GCAS response in this long-time test and the R-square of 0.8788 was obtained. This result demonstrated the feasibility of using the same GCAS sensor chip for long-time continuous transdermal biomarker tracking.

4. Conclusions

We have developed a wearable sensing system for detecting transdermal volatile biomarkers related to dietary macronutrients intake using the gradient based colorimetric array sensor (GCAS). The system comprising 1) a sensor chip that can localize the color development associated with the chemical reaction between the transdermal volatile biomarkers and the porous sensing probes; and 2) an optical detection system that can record and process the optical signal caused by the localized color development to quantitatively determine the emission rates of the transdermal volatile biomarkers. The GCAS sensor chip consists of an array of gradient sensing channels, allowing multiplexed detection of multiple transdermal volatile biomarkers simultaneously. The detection can be achieved in two ways: 1) processing the optical images of the GCAS before and after the volatile biomarkers exposure; 2) processing the real-time optical signal of the GCAS during the volatile biomarkers exposure for continuous monitoring. The performance of the GCAS-based wearable sensing systems for transdermal volatile acetone tracking has been validated by testing human subjects in both offline and online modes in diet-control pilot studies. A good correlation between the transdermal acetone and breath acetone (in the range of 0–40 ppm) has been observed and the R square is as high as 0.8877. The GCAS sensor chip also shows the capacity for long-time continuous tracking of transdermal biomarkers. Compared to the conventional self-reporting approach and blood or breath analysis methods, this GCAS technique provides a noninvasive, low-cost, and wearable tool for reliable assessment of dietary macronutrients intake outside of lab or hospital settings. Besides the advantages of this sensing technique, several challenges need to be addressed before applying the GCAS sensor in practical applications, such as developing more sensitive and selective colorimetric sensing recipes to reduce the response time and improve the reliability of the sensor, and investigating the long-term stability and shelf life of the sensor. More clinical studies are also needed to investigate the influence of differences of skin gas permeability on the sensor performance. We hope this wearable and user-friendly dietary macronutrients intake technique could play an important role in helping doctors and patients to effectively manage metabolism-related diseases in the future.

CRediT authorship contribution statement

Jingjing Yu: Investigation, Methodology, Data curation, Validation, Formal analysis, Visualization, Writing – review & editing. **Di Wang:** Funding acquisition, Conceptualization, Investigation, Methodology, Data curation, Formal analysis, Writing – review & editing. **Vishal Varun Tipparaju:** Methodology. **Wonjong Jung:** Funding acquisition. **Xiaojun Xian:** Funding acquisition, Conceptualization, Project administration, Supervision, Resources, Methodology, Formal analysis, Writing – original draft, Writing – review & editing.

Declaration of competing interest

The authors declare that they have no known competing financial interests or personal relationships that could have appeared to influence the work reported in this paper.

Acknowledgement

This project was supported by Samsung Advanced Institute of Technology (SAIT) at Samsung Electronics Co. Ltd (South Korea) under the GRO Research Agreement. We would like to thank Dr. Nongjian Tao for his advice on the project. We would also like to thank Dr. Francis Tsow for his suggestions on the electrical engineering aspect of the sensing system.

Appendix A. Supplementary data

Supplementary data to this article can be found online at https://doi.org/10.1016/j.bios.2021.113650.

References

Alhazmi, A., Stojanovski, E., McEvoy, M., Garg, M.L., 2012. Macronutrient intakes and development of type 2 diabetes: a systematic review and meta-analysis of cohort studies. J. Am. Coll. Nutr. 31 (4), 243–258.
Amann, A., Costello, B.e.L., Miekisch, W., Schubert, J., Buszewski, B., Pleil, J., Ratcliffe, N., Risby, T., 2014. The human volatilome: volatile organic compounds (VOCs) in exhaled breath, skin emanations, urine, feces and saliva. J. Breath Res. 8 (3), 034001.
Anderson, J.C., 2015. Measuring breath acetone for monitoring fat loss. Obesity 23 (12), 2327–2334.
Astrup, A., 1999. Macronutrient balances and obesity: the role of diet and physical activity. Publ. Health Nutr. 2 (3a), 341–347.
Avallone, E.V., De Carolis, A., Loizos, P., Corrado, C., Vernia, P., 2010. Hydrogen breath test–diet and basal H2 excretion: a technical note. Digestion 82 (1), 39–41.
Basiotis, P.P., Welsh, S.O., Cronin, F.J., Kelsay, J.L., Mertz, W., 1987. Number of days of food intake records required to estimate individual and group nutrient intakes with defined confidence. J. Nutr. 117 (9), 1638–1641.
Bridgeman, D.T., 2017. A Portable Colorimetric Sensing Platform for the Evaluation of Carbon Dioxide in Breath. Arizona State University.
Combs, G.F., Trumbo, P.R., McKinley, M.C., Milner, J., Studenski, S., Kimura, T., Watkins, S.M., Raiten, D.J., 2013. Biomarkers in nutrition: new frontiers in research and application. Ann. N. Y. Acad. Sci. 1278, 1–10.
Darby, A., Strum, M.W., Holmes, E., Gatwood, J., 2016. A review of nutritional tracking mobile applications for diabetes patient use. Diabetes Technol. Therapeut. 18 (3), 200–212.
Douwes, A., Oosterkamp, R., Fernandes, J., Los, T., Jongbloed, A., 1980. Sugar malabsorption in healthy neonates estimated by breath hydrogen. Arch. Dis. Child. 55 (7), 512–515.
Fontana, L., Partridge, L., 2015. Promoting health and longevity through diet: from model organisms to humans. Cell 161 (1), 106–118.
Franceschi, S., La Vecchia, C., Russo, A., Favero, A., Negri, E., Conti, E., Montella, M., Filiberti, R., Amadori, D., Decarli, A., 1998. Macronutrient intake and risk of colorectal cancer in Italy. Int. J. Canc. 76 (3), 321–324.
Gallagher, M., Wysocki, C.J., Leyden, J.J., Spielman, A., Sun, X., Preti, G., 2008. Analyses of volatile organic compounds from human skin. Br. J. Dermatol. 159 (4), 780–791.
Ghoshal, U.C., 2011. How to interpret hydrogen breath tests. Journal of neurogastroenterology and motility 17 (3), 312.
Gibbons, H., Brennan, L., 2017. Metabolomics as a tool in the identification of dietary biomarkers. Proc. Nutr. Soc. 76 (1), 42–53.
Güntner, A.T., Kompalla, J.F., Landis, H., Theodore, S.J., Geidl, B., Sievi, N.A., Kohler, M., Pratsinis, S.E., Gerber, P.A., 2018. Guiding ketogenic diet with breath acetone sensors. Sensors 18 (11), 3655.
Havlicek, J., Saxton, T.K., 2009. The Effect of Diet on Human Bodily Odors. New Research on Food Habits. Nova Science Publishers, pp. 35–44.
Hedrick, V.E., Dietrich, A.M., Estabrooks, P.A., Savla, J., Serrano, E., Davy, B.M., 2012. Dietary biomarkers: advances, limitations and future directions. Nutr. J. 11, 109.
Hu, J., La Vecchia, C., Negri, E., de Groh, M., Morrison, H., Mery, L., 2015. Macronutrient intake and stomach cancer. Cancer Causes Control 26 (6), 839–847.
Kereliuk, S.M., Brawerman, G.M., Dolinsky, V.W., 2017. Maternal macronutrient consumption and the developmental origins of metabolic disease in the offspring. Int. J. Mol. Sci. 18 (7), 1451.
King, J., Mochalski, P., Kupferthaler, A., Unterkofler, K., Koc, H., Filipiak, W., Teschl, S., Hinterhuber, H., Amann, A., 2010. Dynamic profiles of volatile organic compounds

in exhaled breath as determined by a coupled PTR-MS/GC-MS study. Physiol. Meas. 31 (9), 1169.
Kondo, T., Tsuda, T., Nose, K., Ishiguro, H., Mitsui, T., Gao, K.P., Fujiki, K., 2002. Assessment of colonic fermentation by hydrogen release from skin. Am. J. Gastroenterol. 97 (5), 1271–1272.
Kotler, D.P., Holt, P.R., Rosensweig, N.S., 1982. Modification of the breath hydrogen test: increased sensitivity for the detection of carbohydrate malabsorption. J. Lab. Clin. Med. 100 (5), 798–805.
Landini, B.E., Bravard, S.T., 2009. Breath acetone concentration measured using a palm-size enzymatic sensor system. IEEE Sensor. J. 9 (12), 1802–1807.
Lin, C.W., Zhu, Y., Yu, J.J., Qin, X.C., Xian, X.J., Tsow, F., Forzani, E.S., Wang, D., Tao, N. J., 2018. Gradient-based colorimetric sensors for continuous gas monitoring. Anal. Chem. 90 (8), 5375–5380.
Lupton, J.R., Brooks, J., Butte, N., Caballero, B., Flatt, J., Fried, S., 2002. Dietary Reference Intakes for Energy, Carbohydrate, Fiber, Fat, Fatty Acids, Cholesterol, Protein, and Amino Acids, vol. 5. National Academy Press, Washington, DC, USA, pp. 589–768.
Macdiarmid, J., Blundell, J., 1998. Assessing dietary intake: Who, what and why of under-reporting. Nutr. Res. Rev. 11 (2), 231–253.
Mochalski, P., King, J., Unterkofler, K., Hinterhuber, H., Amann, A., 2014. Emission rates of selected volatile organic compounds from skin of healthy volunteers. J. Chromatogr. B 959, 62–70.
Musa-Veloso, K., Likhodii, S.S., Cunnane, S.C., 2002. Breath acetone is a reliable indicator of ketosis in adults consuming ketogenic meals. Am. J. Clin. Nutr. 76 (1), 65–70.
Muzio, F., Mondazzi, L., Harris, W.S., Sommariva, D., Branchi, A., 2007. Effects of moderate variations in the macronutrient content of the diet on cardiovascular disease risk factors in obese patients with the metabolic syndrome. Am. J. Clin. Nutr. 86 (4), 946–951.
Naitoh, K., Tsuda, T., Nose, K., Kondo, T., Takasu, A., Hirabayashi, T., 2002. New measurement of hydrogen gas and acetone vapor in gases emanating from human skin. Instrum. Sci. Technol. 30 (3), 267–280.
Natarajan, L., Pu, M., Fan, J., Levine, R.A., Patterson, R.E., Thomson, C.A., Rock, C.L., Pierce, J.P., 2010. Measurement error of dietary self-report in intervention trials. Am. J. Epidemiol. 172 (7), 819–827.
Nose, K., Mizuno, T., Yamane, N., Kondo, T., Ohtani, H., Araki, S., Tsuda, T., 2005. Identification of ammonia in gas emanated from human skin and its correlation with that in blood. Anal. Sci. 21 (12), 1471–1474.
Organization, W.H., 2003. Diet, Nutrition, and the Prevention of Chronic Diseases: Report of a Joint WHO/FAO Expert Consultation. World Health Organization.
Petrus, M., Bratu, A., Popa, C., 2017. Spectroscopic study of dietary effects on volatile breath biomarkers. Rom. Rep. Phys. 69 (609), 2020.
Potischman, N., 2003. Biologic and methodologic issues for nutritional biomarkers. J. Nutr. 133 (Suppl. 3), 875S–880S.
Prabhakar, A., Quach, A., Wang, D., Zhang, H., Terrera, M., Jackemeyer, D., Xian, X., Tsow, F., Tao, N., Forzanil, E., 2014. Breath acetone as biomarker for lipid oxidation and early ketone detection. Global Journal of Obesity, Diabetes and Metabolic Syndrome 1 (1), 012-019.
Rondanelli, M., Perdoni, F., Infantino, V., Faliva, M.A., Peroni, G., Iannello, G., Nichetti, M., Alalwan, T.A., Perna, S., Cocuzza, C., 2019. Volatile organic compounds as biomarkers of gastrointestinal diseases and nutritional status. Journal of Analytical Methods in Chemistry 2019, 7247802.
Sekine, Y., Toyooka, S., Watts, S.F., 2007. Determination of acetaldehyde and acetone emanating from human skin using a passive flux sampler—HPLC system. J. Chromatogr. B 859 (2), 201–207.
Shirasu, M., Touhara, K., 2011. The scent of disease: volatile organic compounds of the human body related to disease and disorder. J. Biochem. 150 (3), 257–266.
Solon-Biet, S.M., Mitchell, S.J., de Cabo, R., Raubenheimer, D., Le Couteur, D.G., Simpson, S.J., 2015. Macronutrients and caloric intake in health and longevity. J. Endocrinol. 226 (1), R17–R28.
Spacek, L.A., Strzepka, A., Saha, S., Kotula, J., Gelb, J., Guilmain, S., Risby, T., Solga, S. F., 2018. Repeated measures of blood and breath ammonia in response to control, moderate and high protein dose in healthy men. Sci. Rep. 8 (1), 2554.
Tao, N., Wang, D., Lin, C., 2019. Method and apparatus for continuous gas monitoring using micro-colorimetric sensing and optical tracking of color spatial distribution. U. S. Patent Application No. 16/142,463.
Yamada, Y., Hiyama, S., Toyooka, T., Takeuchi, S., Itabashi, K., Okubo, T., Tabata, H., 2015. Ultratrace measurement of acetone from skin using Zeolite: toward development of a wearable monitor of fat metabolism. Anal. Chem. 87 (15), 7588–7594.
Yamane, N., Tsuda, T., Nose, K., Yamamoto, A., Ishiguro, H., Kondo, T., 2006. Relationship between skin acetone and blood β-hydroxybutyrate concentrations in diabetes. Clin. Chim. Acta 365 (1–2), 325–329.